

Removal of cationic dyes by kaolinite

M. Hamdi Karaoğlu^a, Mehmet Doğan^{b,*}, Mahir Alkan^b

^a Muğla University, Faculty of Science and Literature, Department of Chemistry, Muğla, Turkey

^b Balıkesir University, Faculty of Science and Literature, Department of Chemistry, 10145 Balıkesir, Turkey

ARTICLE INFO

Article history:

Received 3 August 2008

Received in revised form 25 January 2009

Accepted 1 February 2009

Available online 20 February 2009

Keywords:

Adsorption

Dyes

Isotherm

Enthalpy

ABSTRACT

The removal of cationic dyes such as maxilon yellow 4GL (MY 4GL) and maxilon red GRL (MR GRL) on kaolinite from aqueous solutions has been studied according to the adsorption method. The adsorbed amount of dyes on kaolinite surface was investigated as a function of pH, ionic strength, temperature, acid activation, and calcination temperature. It was found that: (i) the adsorbed amount of cationic dyes increased with increase in pH and decreased with increase in temperature, ionic strength, acid activation, and calcination temperature; (ii) the adsorption process was an exothermic process; (iii) the experimental data were correlated reasonably well by the adsorption isotherm of the Langmuir; and (iv) the interactions between adsorbate and adsorbent from adsorption heat data were physical in nature.

© 2009 Elsevier Inc. All rights reserved.

1. Introduction

Colored organic effluents are produced in the textile, paper, plastic, leather, food, and mineral processing industries [1,2]. Wastewater containing pigments and/or dyes can cause serious water pollution problems. In addition, dyes are toxic to some organisms and hence, harmful to aquatic animals. Furthermore, the expanded uses of dyes have shown that some of them and their reaction products, such as aromatic amines, are highly carcinogenic [1,3]. Therefore, removal of dyes before disposal of wastewater is necessary. In general, there are five main methods used for the treatment of dye-containing effluent: adsorption, oxidation–ozonation, biological treatment, coagulation–flocculation, and membrane processes [4,5].

The adsorption process is one of the most efficient methods of removing pollutants from wastewater. The ability of adsorption to remove toxic chemicals without disturbing the quality of water or leaving behind any toxic degraded products has augmented its usage in comparison to electrochemical, biochemical or photochemical degradation processes [6,7]. Recovery of costly toxic substances from the wastewater is an added advantage of the adsorption procedure. Also, the adsorption process provides an attractive alternative treatment, especially if the adsorbent is inexpensive and readily available [8]. Activated carbon has been widely used as an adsorbent for the removal of various pollutants due to its high adsorption capacity. However, it has relatively high operation costs, regeneration problems, and is difficult to separate it

from the wastewater after use. Therefore, a number of low-cost adsorbents have been tried for treatment of wastewaters [9]. A wide variety of materials, such as clay minerals [10], activated carbon, bagasse pith [11], wood [12], maize cob [13], and peat [14], are being evaluated as viable adsorbents to remove dyes from colored effluents. However, the adsorption capacity of the adsorbents is not very large. For the past few years, the focus of the research is to utilize cheap materials as potential adsorbents and the processes developed so far are based on exploring those solid waste products, which can prove economic and bring cost effectiveness [7].

Kaolinite is one of the most common phyllosilicate clay minerals with the chemical composition $\text{Al}_2\text{Si}_2\text{O}_5(\text{OH})_4$. It is a layered silicate mineral, with one tetrahedral sheet linked through oxygen atoms to one octahedral sheet of alumina octahedra. Successive 1:1 layers are held together by hydrogen bonding of adjacent silica and alumina layers. The tetrahedral sheet carries a small permanent negative charge due to isomorphous substitution of Si^{4+} by Al^{3+} , leaving a single-negative charge for each substitution. Both the octahedral sheet and the crystal edges have a pH-dependent variable charge caused by protonation and deprotonation of surface hydroxyl (SOH) groups. Kaolinite has a low shrink–swell capacity and a low cation exchange capacity (1–15 meq/100 g). It is a soft, earthy, usually white mineral. Kaolin is used in ceramics, medicine, coated paper, as a food additive, in toothpaste, as a light diffusing material in white incandescent light bulbs, and in cosmetics. It is also used in most paints and inks. The largest use is in the production of paper [15–18].

In our previous works, we have investigated the electrokinetic properties of kaolinite suspensions [19]; and also the adsorption

* Corresponding author. Tel.: +90 266 612 10 00; fax: +90 266 612 12 15.

E-mail addresses: mdogan@balikesir.edu.tr, mdogan7979@yahoo.com (M. Doğan).

of copper (II) from aqueous solutions onto kaolinite samples [16]. In this study, kaolinite, which is a low-cost adsorbent for the removal of dyes, was studied for its potential use as an adsorbent for removal of cationic dyes such as maxilon yellow 4GL (MY 4GL) and maxilon red GRL (MR GRL) from aqueous solution. Effects of different parameters such as pH, ionic strength, acid activation, calcination temperature and solution temperature on adsorption equilibrium were studied. The experimental data for adsorbed MY 4GL and MR GRL on kaolinite were compared using two isotherm equations namely, Freundlich and Langmuir. In addition, the equilibrium thermodynamic parameters are determined for MY 4GL and MR GRL on kaolinite.

2. Material and methods

2.1. Materials

The kaolinite sample was obtained from Guzelyurt (Aksaray, Turkey). All chemicals used were of analytical reagent grade and were used without further purification. The chemical structures of MY 4GL and MR GRL are illustrated in Fig. 1. The cation exchange capacity (CEC) of kaolinite was determined by the ammonium acetate method [20]. The some physicochemical properties and chemical composition of kaolinite are given in Tables 1 and 2 [16,19].

2.2. Purification of kaolinite

Kaolinite was treated before using in the experiments as follows [21]: the aqueous suspension containing 10 g/L kaolinite was mechanically stirred for 24 h, after waiting for about 2 min the supernatant suspension was filtered through a white-band filter paper (Φ (diameter of filter paper) = 12.5 cm). The solid sample was dried at 110 °C for 24 h, then sieved by 100-mesh sieve. The particles under 100-mesh are used in further experiments.

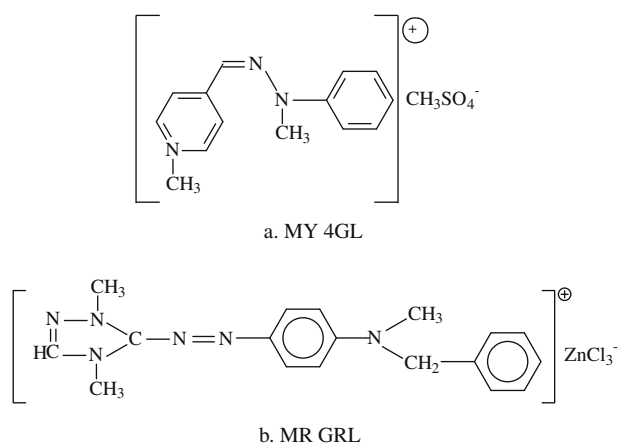


Fig. 1. Structures of dyes.

Table 1
Some physicochemical properties of kaolinite.

Color	White
Cation exchange capacity (meq/100 g)	13.00
Density (g/mL)	2.18
pH	7.90
Specific surface area (m ² /g)	17
Hardness (kg/mm ²)	2–3

Table 2
Chemical composition of kaolinite.

Constituent	Weight (%)
SiO ₂	53.00
Al ₂ O ₃	26.71
Na ₂ O	0.62
K ₂ O	1.39
CaO	0.57
Fe ₂ O ₃	0.37
MgO	0.28
Loss of ignition	17.20

2.3. Acid Activation of kaolinite

In order to obtain the acid activated kaolinite samples H₂SO₄ solutions were used. The aqueous suspensions of kaolinite in 0.2, 0.4, and 0.6 M H₂SO₄ solutions (so that acid/solid ratios were 1/5, 2/5, and 3/5 g/g) were refluxed with a reflux apparatus, then filtered and dried at 110 °C for 24 h [20].

2.4. Calcination of kaolinite

Kaolinite samples were ground after the cleaning mechanically from its visible impurities, and sieved to obtain 0–100 μm size fraction. Then, they were dried at 110 °C, and used in the experiments. Calcinated kaolinite samples have been prepared in the temperature range of 110–800 °C with a Nuve MF-140 furnace [16]. A simultaneous DTA/TG system was used for differential thermal (DTA) and thermogravimetric (TG) analysis (Perkin–Elmer Diamond DTA/TG).

2.5. Adsorption experiments

All the adsorption studies were carried out by batch technique. Batch adsorption studies were performed at different pH, ionic strengths and temperatures to obtain equilibrium isotherms. The initial concentrations of MY 4GL and MR GRL dyes in the experiments are in the range of 1–90 × 10⁻⁵ and 1–30 × 10⁻⁵ mol/L, respectively. The dye solution (50 mL) of desired concentration at natural pH was taken in polyethylene flasks and agitated with a known weight of kaolinite at room temperature (30 ± 0.5 °C) in a shaker water bath at 120 1/min for the desired time periods, up to a maximum of about 3 h. Preliminary experiments demonstrated that the equilibrium was established in 3 h. Equilibration for longer times gave practically the same uptake. Therefore, a contact period of 3 h was finally selected for all of the equilibrium tests. A thermostated shaker bath was used to keep the temperature constant. The solution pH was carefully adjusted by adding a small amount of HCl or NaOH solution and measured using an Orion 920A pH-meter equipped with a combined pH electrode. pH-meter was standardized with NBS buffers before every measurement. The effect of ionic strength was investigated at 0.001–0.100 mol/L KCl salt concentrations. The sorption studies were also carried out at different temperatures, i.e., 30, 40, 50, and 60 °C, to determine the effect of temperature and to evaluate the adsorption thermodynamic parameters. At the end of the adsorption period, the solution was centrifuged for 15 min at 3000 1/min and then the concentrations of the residual dyes, C_e, were determined. Initial and final dye concentrations were determined using a Perkin–Elmer Lambda 25 UV–vis spectrophotometer corresponding to λ_{max} of each dye (410 and 531 nm for MY 4GL and MR GRL, respectively). Concentrations of dyes in solution were estimated quantitatively using the linear regression equations obtained by plotting a calibration curve for each dye over a range of concentrations. Blanks containing no dyes were used for each series of experiments. Each experiment data was an average of two independent

adsorption tests. The amount of dye adsorbed at equilibrium, q_e was calculated from the mass balance equation:

$$q_e = (C_0 - C_e) \frac{V}{W} \quad (1)$$

where C_0 and C_e are the initial and equilibrium liquid-phase concentrations of dye solution (mol/L), respectively; q_e is equilibrium dye concentration on adsorbent (mol/g), V is the volume of dye solution (L), and W is the mass of kaolinite sample used (g) [22].

3. Results and discussion

3.1. Adsorption equilibrium and parameters

3.1.1. Effect of pH

The removal of MY 4GL and MR GRL dyes as a function of pH is shown in Fig. 2. The results reveal that the adsorption of the dyes increases with an increase in pH of the solution from 3.0 to 9.0. The shapes of the isotherms in Fig. 2 show a plateau corresponding to monolayer formation of adsorbed molecules on the surface which is a result of Langmuir isotherm. For clay minerals the potential determining ions are H^+ and OH^- and complex ions formed by bonding with H^+ and OH^- . The broken Si–O bonds and Al–OH bonds along the surfaces of the clay crystals result in hydrolysis [23]. The silicon atoms at the surface tend to maintain their tetrahedral coordination with oxygen. They complete their coordination at room temperature by attachment to monovalent hydroxyl groups, forming silanol groups. Theoretically, it is possible to use a pattern in which one silicon atom bears two or three hydroxyl

groups, yielding silanediol and silanetriol groups, respectively. It is stated as improbable that silanetriol groups exist at the silica surface [19,21]. We previously found that kaolinite had a pH_{zpc} at pH 2.35 [19]. The surface is positive at lower pH than pH_{zpc} where reaction (2) predominates, and is negative at higher pH than pH_{zpc} when reaction (3) takes over:



At $pH = pH_{zpc}$

$$[\equiv SO^-] = [\equiv SOH_2^+] \quad (4)$$

where S shows Al, Si atoms. As the pH of the suspension increases according to Eq. (3), the association of dye cations with more negatively charged kaolinite surface can easily take place due to electrostatic attraction as following reaction:



On the other hand, at the lower pH values from pH_{zpc} , the adsorption of dyes decreases due to competing between dye cations and hydrogen ions for the adsorption sites. A similar effect was previously reported by Mall and Upadhyay for methylene blue adsorption on fly ash particles [24] and Dogan and Alkan for methyl violet adsorption on perlite [25].

3.1.2. Effect of ionic strength

Extensive investigations carried out on adsorption of dyes revealed that the extent of dye uptake was strongly influenced by the concentration and nature of the electrolyte ionic species added to the dye bath [26]. There are a number of studies, which show an important effect on the removal extent of dyes with the concentration and nature of various electrolyte types in dye system [27–30]. The presence of salt (KCl) in the solution may have two opposite effects. On the one hand, since the salt screens the electrostatic interaction of opposite charges of the oxide surface and the dye molecules, the adsorbed amount should decrease with increase of KCl concentration. On the other hand, the salt causes an increase in the degree of dissociation of the dye molecules by facilitating the protonation [29–31].

Furthermore, ionic strength is one of the key factors affecting the electrical double layer (EDL) structure of a hydrated particulate. An increasing in the ionic strength could lead to a decrease in the thickness of the EDL, thereby resulting in a decrease in adsorption. The thickness of EDL, $1/\kappa$, can be determined from the relationship:

$$\frac{1}{\kappa} = \left(\frac{2F^2 \cdot I \cdot 1000}{\epsilon \cdot \epsilon_0 \cdot RT} \right)^{-0.5} \quad (6)$$

where $1/\kappa$ is the reciprocal Debye length of EDL (m); F is the Faraday constant (C/mol); I is the ionic strength (mol/L); R is the molar gas constant (J/(mol K)); T is the absolute temperature (K); ϵ is the dielectric constant of water; and ϵ_0 is the vacuum permittivity (C/(V m)) [9,19].

Fig. 3 shows the influence of ionic strength to adsorption extent of MY 4GL and MR GRL on kaolinite. As indicated by Eq. (6), an increase in ionic strength would lead to a decrease in $1/\kappa$ and increase the amount of indifferent ions approaching to kaolinite surface. Thus, the results shown in Fig. 3 can be attributed to salt screening effect and also the decrease in the thickness of EDL as the ionic strength increases.

3.1.3. Effect of acid activation

The effect of acid activation on the adsorption of MY 4GL and MR GRL dyes on kaolinite has been given in Fig. 4. The adsorbed

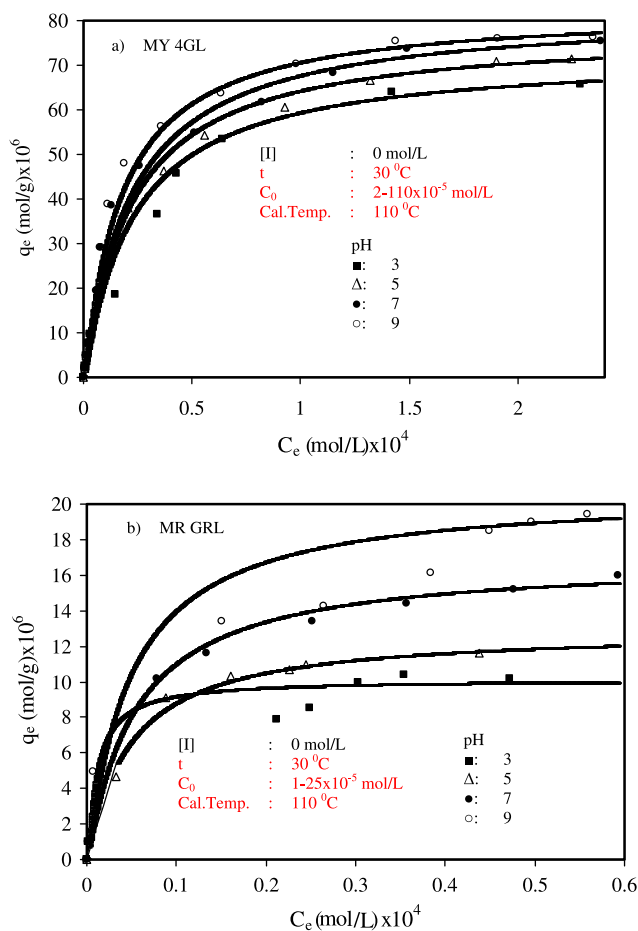


Fig. 2. Effect of initial pH on adsorption of MY 4GL and MR GRL onto kaolinite.

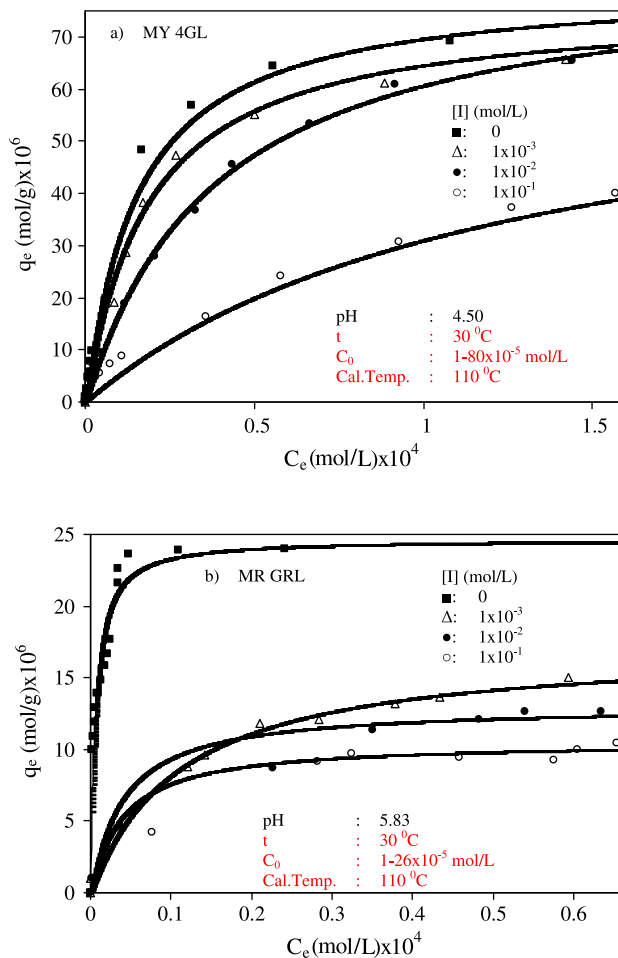


Fig. 3. Effect of ionic strength on adsorption of MY 4GL and MR GRL onto kaolinite.

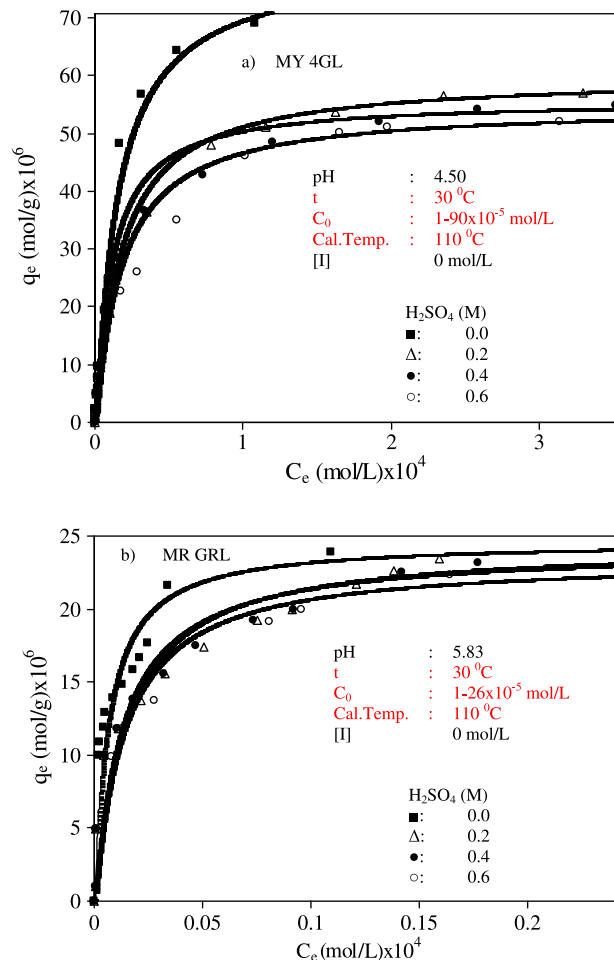


Fig. 4. Effect of acid activation on adsorption of MY 4GL and MR GRL onto kaolinite.

amounts of dye ions decreased with the increasing concentration of H_2SO_4 used for the acid activation. This may be due to the partial destruction of kaolinite structure, as was shown by González-Pradas et al. [32] and López-González and González-García [33] for bentonite, and also may be due to transforming of SOH groups to SOH_2^+ groups on kaolinite surface. As can be seen in Fig. 4, the data converge to a horizontal plateau. This plateau corresponds to the formation of a monolayer of adsorbate on the kaolinite.

3.1.4. Effect of calcination temperature

Fig. 5 has shown the adsorption of MY 4GL and MR GRL dyes onto calcinated and natural kaolinite samples. The shape of curves progresses towards a constant covered fraction, which shows a monolayer of adsorbate on the adsorbent. As can be seen in this figure, the amount of the adsorbed dyes on kaolinite has decreased with increasing calcination temperature. Fig. 6 shows DTA/TG curves of kaolinite. The DTA peak temperatures are characteristic for each mineral and DTA curves are applicable for the identification and determination of many clays [34,35]. It can be seen that at nearly 530°C , there is an endothermic peak corresponding to the dehydroxylation of kaolinite and the formation of metakaolinite. At nearly 1016°C , an exothermic peak is related to crystallization of Al-Si spinel phase at the medium scale of temperature [36]. As seen from TG curve in Fig. 6, dehydroxylation of kaolinite results in about 11.4% mass loss. During calcination, the silicon atoms experience a range of environments of differing distortion due to dehydroxylation. In our previous works, we found that the intensity of hydroxyl peaks decreased with increase

in calcination temperature [16]. Therefore, the decrease in the amount adsorbed of MY 4GL and MR GRL dyes with increasing calcination temperature may be a result of the removal of most of the micropores due to the calcination of sample [37] and due to the decrease in OH groups in kaolinite during the calcination process.

3.1.5. Adsorption temperature

A study of the temperature dependence of adsorption reactions gives valuable knowledge about the enthalpy and entropy changes during adsorption. When the adsorption was carried out at four different temperatures from 30 to 60°C with an interval of 10°C , the extent of adsorption decreased with an increase in adsorption temperature for both dyes as seen in Fig. 7, indicating that the process is an exothermic. The fact that the adsorption capacity of kaolinite for MY 4GL and MR GRL tends to decrease with increase in temperature shows that the adsorption process occurs as a physisorption indicating that adsorption arises from the weaker van der Waals and dipole forces which are usually associated with low heat of adsorption. Moreover, careful examination of Fig. 7, in particular at high temperatures, reveals that desorption might be occurring. This behavior could be attributed to either a reversible adsorption or a back diffusion controlling mechanism [38].

3.2. Adsorption isotherm

The equilibrium adsorption isotherm is of importance in the design of adsorption systems. The isotherm assumes that adsorbent

surface sites have a spectrum of different binding energies. In general, the adsorption isotherm describes how adsorbates interact with adsorbents. Thus, the correlation of equilibrium data by either a theoretical or an empirical equation is essential to the practical

design and operation of an adsorption system. Several isotherm equations are available, and two important isotherms were selected for this study: the Langmuir and Freundlich isotherms. The Langmuir and Freundlich equations are commonly used to

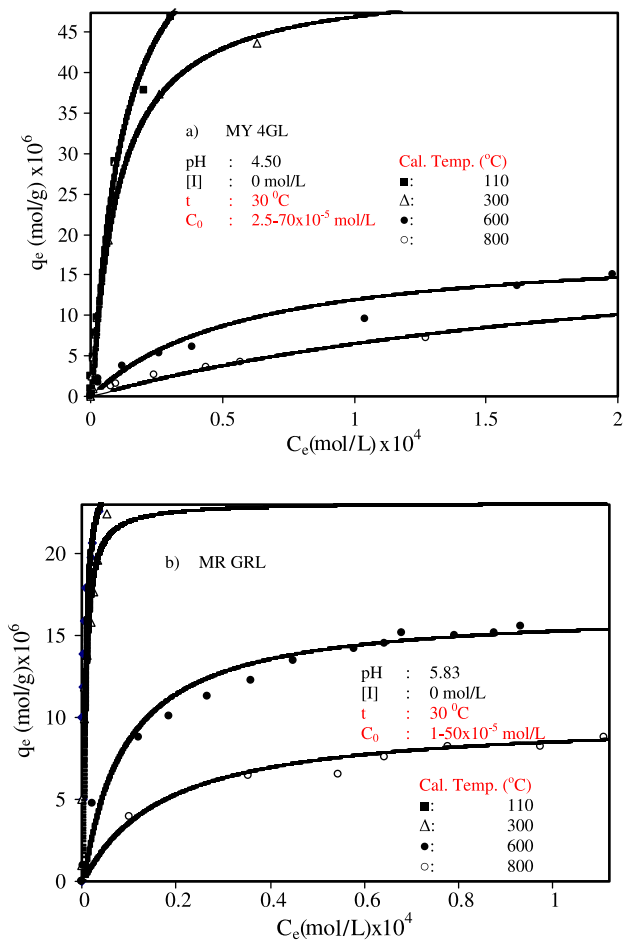


Fig. 5. Effect of calcination temperature on adsorption of MY 4GL and MR GRL onto kaolinite.

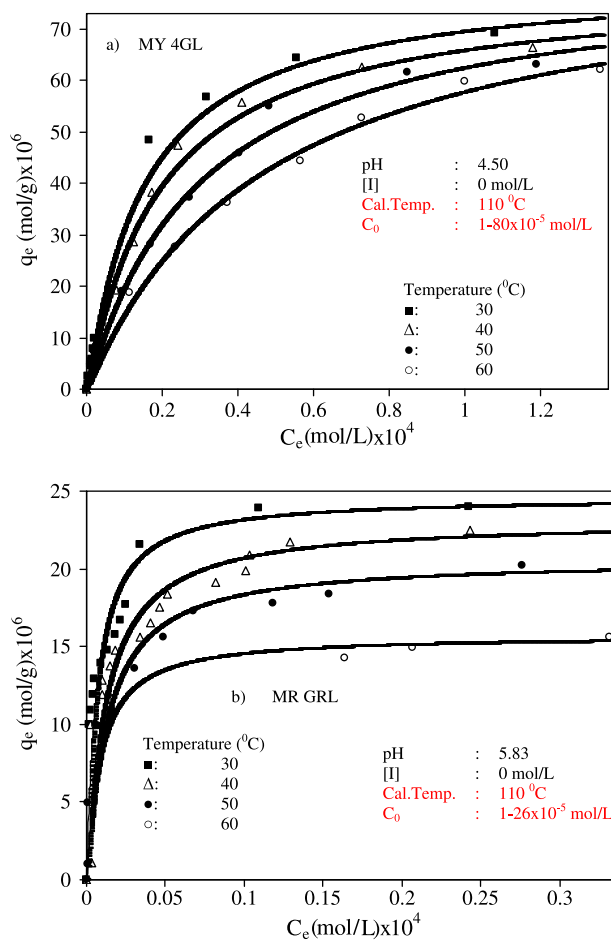


Fig. 7. Effect of adsorption temperature on adsorption of MY 4GL and MR GRL onto kaolinite.

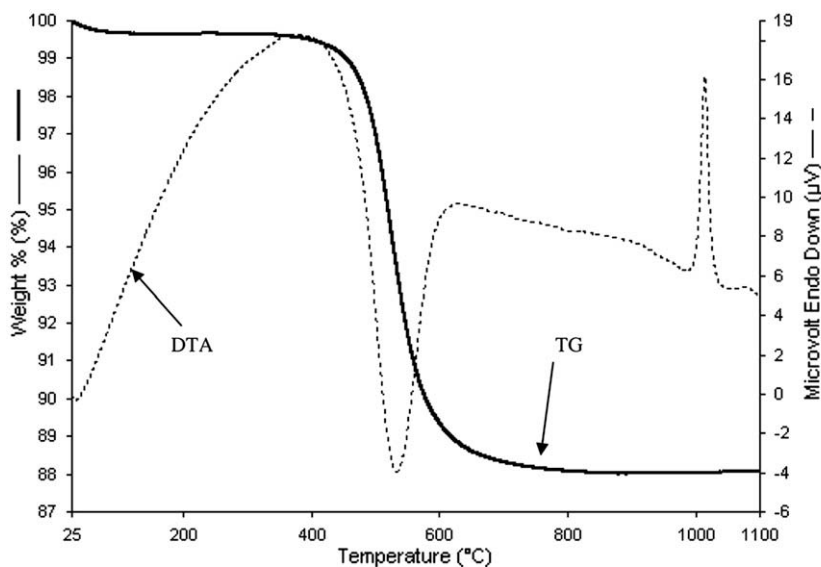


Fig. 6. DTA and TG spectrums of kaolinite under nitrogen atmosphere.

describe adsorption isotherms at a constant temperature for water and wastewater treatment applications [1,39,40].

3.2.1. Freundlich isotherm

The Freundlich isotherm is the earliest known relationship describing the adsorption equation. This fairly satisfactory empirical isotherm can be used for nonideal adsorption that involves heterogeneous surface energy systems [41]. The Freundlich isotherm is commonly given by

$$q_e = K_F C_e^{1/n} \tag{7}$$

$$\ln q_e = \ln K_F + \frac{1}{n} \ln \left(\frac{C_e}{C_0} \right) \tag{8}$$

where K_F is a Freundlich constant that shows both the adsorption capacity of an adsorbent and the strength of the relationship between adsorbate and adsorbent. The slope $1/n$, ranging between 0 and 1, is a measure of adsorption intensity or surface heterogeneity, becoming more heterogeneous as its value gets closer to zero. In general, as K_F increases the adsorption capacity of an adsorbent

for a given adsorbate increases. K_F and $(1/n)$ can be determined from the linear plot of $\ln q_e$ vs. $\ln C_e$ [40].

3.2.2. Langmuir isotherm

Langmuir isotherm equation has been widely applied to describe experimental adsorption data. The Langmuir equation assumes that there is no interaction between the sorbate molecules and that the sorption is localized in a monolayer. It is then assumed that once a dye molecule occupies a site, no further sorption can take place at that site. The well known expression of the Langmuir model is given by Eq. (9) or (10):

$$q_e = \frac{q_m K C_e}{1 + K C_e} \tag{9}$$

$$\frac{C_e}{q_e} = \frac{1}{q_m K} + \frac{1}{q_m} \cdot C_e \tag{10}$$

where q_e (mol/g) and C_e (mol/L) are the amount of adsorbed dye per unit weight of adsorbent and unadsorbed dye concentration in solution at equilibrium, respectively. q_m is the maximum amount of the

Table 3
Isotherm constants for MY 4GL adsorption on kaolinite.

Parameters					Langmuir isotherm				Freundlich isotherm
Adsorption temperature (°C)	H ₂ SO ₄ (M)	Calcination temperature (°C)	pH	[I] (mol/L)	q_m (mol/g) × 10 ⁵	K (L/mol) × 10 ⁻⁴	R ²	R _L	R ²
30			4.50	0	7.97	6.57	0.994	0.9–0.123	0.963
40			4.50	0	7.86	5.13	0.993	0.9–0.141	0.952
50			4.50	0	8.14	3.28	0.993	0.9–0.203	0.959
60			4.50	0	8.53	2.09	0.991	0.9–0.260	0.938
30			4.50	0.001	7.43	5.48	0.996	0.9–0.113	0.970
30			4.50	0.010	8.16	2.61	0.990	0.9–0.210	0.986
30			4.50	0.100	5.28	0.80	0.978	0.9–0.443	0.982
30			3	0	7.23	4.44	0.996	0.9–0.089	0.971
30			5	0	7.78	4.69	0.998	0.9–0.086	0.967
30			7	0	8.21	4.65	0.996	0.9–0.082	0.915
30			9	0	8.27	5.78	0.998	0.9–0.068	0.807
30		100	4.50	0	6.51	8.65	0.990	0.9–0.100	0.983
30		300	4.50	0	5.15	1.01	0.998	0.9–0.076	0.913
30		600	4.50	0	1.89	1.70	0.993	0.9–0.229	0.990
30		800	4.50	0	2.26	0.40	0.988	0.9–0.577	0.996
30	0.2		4.50	0	5.98	0.58	0.999	0.9–0.049	0.974
30	0.4		4.50	0	5.57	0.92	0.997	0.9–0.029	0.952
30	0.6		4.50	0	5.47	0.57	0.994	0.9–0.052	0.957

Table 4
Isotherm constants for MR GRL adsorption on kaolinite.

Parameters					Langmuir isotherm				Freundlich isotherm
Adsorption temperature (°C)	H ₂ SO ₄ (M)	Calcination temperature (°C)	pH	[I] (mol/L)	q_m (mol/g) × 10 ⁵	K (L/mol) × 10 ⁻⁵	R ²	R _L	R ²
30			5.83	0	2.46	15.72	0.998	0.7–0.025	0.951
40			5.83	0	2.31	8.54	0.995	0.8–0.045	0.972
50			5.83	0	2.06	8.06	0.996	0.9–0.043	0.825
60			5.83	0	1.57	12.30	0.998	0.7–0.023	0.829
30			5.83	0.001	1.72	0.90	0.990	0.9–0.157	0.994
30			5.83	0.010	1.30	2.53	0.995	0.9–0.058	0.996
30			5.83	0.100	1.04	2.57	0.990	0.9–0.056	0.978
30			3	0	1.01	9.53	0.983	0.8–0.021	0.974
30			5	0	1.29	2.14	0.997	0.5–0.095	0.846
30			7	0	1.69	1.87	0.996	0.9–0.082	0.953
30			9	0	2.07	2.09	0.991	0.9–0.078	0.911
30		100	5.83	0	2.56	24.15	0.996	0.6–0.050	0.742
30		300	5.83	0	2.31	19.40	0.999	0.9–0.048	0.859
30		600	5.83	0	1.66	1.11	0.991	0.9–0.088	0.973
30		800	5.83	0	0.99	0.57	0.994	0.9–0.135	0.989
30	0.2		5.83	0	2.44	7.09	0.990	0.9–0.081	0.821
30	0.4		5.83	0	2.41	7.69	0.993	0.9–0.068	0.808
30	0.6		5.83	0	2.34	7.40	0.993	0.9–0.076	0.888

dye bound per unit weight of adsorbent to form a complete monolayer on the surface at high C_e , and K is the equilibrium constant or Langmuir constant related to the affinity of binding sites (L/mol). q_m and K were calculated from the slope and intercept of the straight lines of the plot C_e/q_e vs. C_e [23,42].

3.3. Isotherm analysis

Values of q_m , K , K_f , and n were calculated from the intercept and slope of the plots. The values for q_m , K , K_f , and n are summarized in Tables 3 and 4. The isotherm data were calculated from the least square method and the related correlation coefficients (R^2 values) are given in the same tables. As seen from Tables 3 and 4, Langmuir equation represents the adsorption process very well; the R^2 values were all higher than 0.99, indicating a very good mathematical fit. The fact that Langmuir isotherm fits the experimental data very well may be due to the homogeneous distribution of active sites onto kaolinite surface, since the Langmuir equation assumes that the surface is homogenous [39]. As seen in Tables 3 and 4, the maximum adsorption capacities for MY 4GL and MR GRL onto kaolinite were found to be in the range of 1.89 – 8.53×10^{-5} and 0.99 – 2.56×10^{-5} mol/g, respectively. Maximum adsorption capacities of kaolinite decreased with increasing temperature.

Previously some researchers investigated several adsorbents such as raw perlite, expanded perlite, bentonite, sepiolite, activated carbon for the removal of some dyes from aqueous solutions. By comparison of the results obtained in this study with those in the previously reported works (Table 5) on adsorption capacities of various low-cost adsorbent, it can be stated that our findings are good.

The essential characteristics of the Langmuir isotherm can be expressed by a separation or equilibrium parameter, a dimensionless constant, which is defined by Eq. (11) [45]:

$$R_L = \frac{1}{1 + KC_e} \quad (11)$$

The value of R_L indicates the type of the isotherm to be either unfavorable ($R_L > 1$), linear ($R_L = 1$), favorable ($0 < R_L < 1$) or irreversible ($R_L = 0$). The R_L values were reported in Tables 3 and 4, that show the adsorption behavior of MY 4GL and MR GRL dyes. The values of R_L were found to be in the range of 0–1, indicating that the adsorption process is favorable for both adsorbates. The results given in Tables 3 and 4 show that the adsorption of MY 4GL and MR GRL onto kaolinite is favorable.

3.4. Heat of adsorption

The most useful heat of adsorption is the isosteric heat of adsorption. The magnitude and variation as a function of coverage fraction may reveal information concerning the bonding to the surface. The isosteric heat of adsorption, ΔH^0 , from the adsorption data at various temperatures as a function of coverage fraction ($\theta = q_e/q_m$) can be estimated from the following equation [32]:

Table 5
Comparison with other adsorbents.

Adsorbents	Dyes	$q_m \times 10^4$ (mol/g)	References
Unexpanded perlite	Methylene blue	1.804–7.118	[20]
Expanded perlite	Methylene blue	0.465–0.821	[20]
Bentonite	Methylene blue	1.12–2.27	[43]
Activated carbon	Methylene blue	10	[44]
Sepiolite	Methylene blue	1.63–2.73	[27]
Sepiolite	Methyl violet	0.18–0.26	[27]
Kaolinite	MY 4GL	0.19–0.85	In this study
Kaolinite	MR GRL	0.10–26	In this study

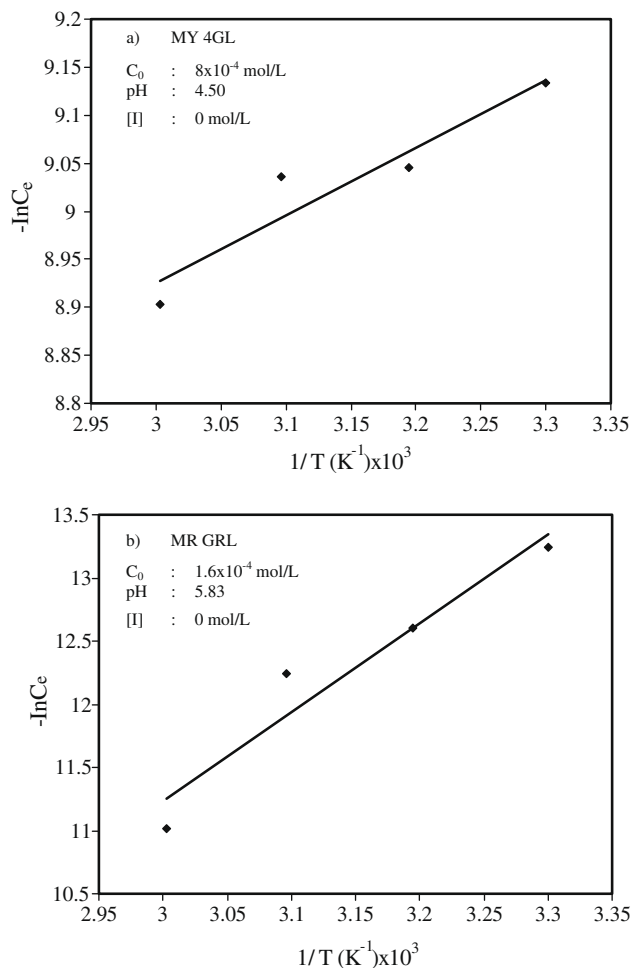


Fig. 8. The plots of $-\ln C_e$ vs. $1/T$.

$$\frac{\Delta H^0}{R} = \left[\frac{\partial(\ln C_e/C_0)}{\partial(1/T)} \right]_{\theta=0.5} \quad (12)$$

where R is the gas constant. Fig. 8 shows the plots of $-\ln C_e$ against $1/T$. The values of ΔH^0 were calculated at a specific coverage fraction of 0.5 as -5.85 kJ/mol for MY 4GL and -58.61 kJ/mol for MR GRL. The value of the enthalpy change indicates that the adsorption is physical in nature involving weak forces of attraction and is also exothermic [46]. Since adsorption is an exothermic process, it would be expected that an increase in solution temperature would result in a decrease in adsorption capacity due to increasing of the desorption rate [26]. Similar result was also found for the adsorption of MB on perlite [20].

4. Conclusions

In this study we investigated the equilibrium of the adsorption of two cationic dyes, which are namely maxilon yellow 4GL and maxilon red GRL onto natural kaolinite. In batch studies, the adsorption increased with increase in solution pH and with decrease in ionic strength, acid activation, calcination temperature and solution temperature. From the obtained data, it was clear that dyes' adsorption mechanisms depend on the adsorbent structure and on the dyes' molecular structure. The experimental equilibrium data obtained were applied to the Langmuir and Freundlich isotherm equations to test the fitness of these equations. By considering the experimental results and adsorption models applied in this study, it can be concluded that adsorption of MY 4GL and

MR GRL dyes obeys Langmuir isotherm, the linearization mode of the Langmuir equation influences the estimation of parameters. The adsorption of MY 4GL and MR GRL onto natural kaolinite was exothermic in nature with the dye removal capacity decreasing with increasing temperature due to increasing mobility of the dye molecules and with increase in desorption rate. The enthalpy change (ΔH^0) for the adsorption process was -5.85 and -58.61 kJ/mol for MY 4GL and MR GRL dyes, respectively, which indicate weak forces between the adsorbed dye molecules and natural kaolinite. The experimental results showed that kaolinite was a suitable adsorbent for removal of MY 4GL and MR GRL dyes.

References

- [1] P.V. Messina, P.C. Schulz, *J. Colloid, Interf. Sci.* 299 (2006) 305–320.
- [2] K.R. Ramakrishna, T. Viraragharan, *Water Sci. Technol.* 36 (1997) 189–192.
- [3] M.F. Boeniger, Carcinogenicity of azo dyes derived from benzidine, Department of Health and Human Services (NIOSH), Cincinnati, Pub. No. 8–119, 1980.
- [4] G. Akkaya, İ. Uzun, F. Güzel, *Dyes Pigments* 73 (2) (2007) 168–177.
- [5] G.M. Walker, L. Hansen, J.A. Hana, S.J. Allen, *Water Res.* 37 (2003) 2081–2089.
- [6] V.K. Gupta, I. Ali, in: A. Hubbard (Ed.), *Adsorbents for Water Treatment: Low-Cost Alternatives to Carbon*, Vol. 1, *Encyclopedia of Surface and Colloid Science*, Marcel Dekker, USA, 2002, pp. 136–166.
- [7] A. Mittal, *J. Hazard. Mater.* B133 (2006) 196–202.
- [8] C. Namasivayam, R. Radhika, S. Suba, *Waste Manag.* 21 (2001) 381–387.
- [9] C.-H. Weng, Y.-F. Pan, *Colloid Surf. A: Physicochem. Eng. Aspects* 274 (2006) 154–162.
- [10] M.M. Nassar, in: *Proceedings of the International Meetings on Chemical Engineering and Biotechnology, IChE-94, Frankfurt, 1994*, pp. 5–11.
- [11] M.M. Nassar, M.S. El-Geundi, *J. Chem. Technol. Biotechnol.* 50 (1991) 257–264.
- [12] H.M. Asfour, O.A. Fadali, M.M. Nassar, M.S. El-Geundi, *J. Chem. Technol. Biotechnol.* 35 (1985) 28–35.
- [13] M.S. El-Geundi, *Water Res.* 25 (3) (1991) 271–273.
- [14] G. McKay, S.J. Allen, *J. Sep. Process Technol.* 4 (3) (1983) 1–10.
- [15] P. Turan, M. Doğan, M. Alkan, *J. Hazard. Mater.* 148 (2007) 56–63.
- [16] M. Alkan, B. Kalay, M. Doğan, O. Demirbas, *J. Hazard. Mater.* 153 (2008) 867–876.
- [17] J. Ikhsan, B.B. Johnson, J.D. Wells, *J. Colloid Interf. Sci.* 217 (1999) 403–410.
- [18] D. Ghosh, K.G. Bhattacharyya, *Appl. Clay Sci.* 20 (2002) 295–300.
- [19] M. Alkan, O. Demirbas, M. Doğan, *Micropor. Mesopor. Mater.* 83 (2005) 51–59.
- [20] M. Doğan, M. Alkan, Y. Onganer, *Water Air Soil Pollut.* 120 (2000) 229–248.
- [21] M. Doğan, M. Alkan, U. Cakir, *J. Colloid, Interf. Sci.* 192 (1997) 114–118.
- [22] O. Demirbas, M. Alkan, M. Doğan, *Adsorption* 8 (2002) 341–349.
- [23] S.S. Tahir, N. Rauf, *Chemosphere* 63 (2006) 1842–1848.
- [24] I.D. Mall, S.N. Upadhyay, *J. Ind. Pulp Paper Technol. Assoc.* 7 (1) (1995) 51–57.
- [25] M. Doğan, M. Alkan, *J. Colloid, Interf. Sci.* 267 (2003) 32–41.
- [26] M. Alkan, M. Doğan, *J. Colloid, Interf. Sci.* 243 (2001) 280–291.
- [27] M. Doğan, Y. Özdemir, M. Alkan, *Dyes Pigments* 75 (2007) 701–713.
- [28] Y. Ozdemir, M. Doğan, M. Alkan, *Micropor. Mesopor. Mater.* 96 (2006) 419–427.
- [29] F. Blockhaus, J.M. Sequaris, H.D. Narres, M.J. Schwuger, *J. Colloid, Interf. Sci.* 186 (1997) 234–247.
- [30] K. Vermohlen, H. Lewandowski, H.D. Narres, M.J. Schwuger, *Colloid Surf. A* 163 (2000) 45–53.
- [31] N. Tekin, O. Demirbas, M. Alkan, *Micropor. Mesopor. Mater.* 85 (3) (2005) 340–350.
- [32] E. González-Pradas, M. Villafranca-Sánchez, M. Socias-Viciana, F. del-Rey-Bueno, A. García-Rodríguez, *J. Chem. Tech. Biotechnol.* 39 (1987) 19–27.
- [33] J.D. López-González, S. González-García, *An. Fis. Quim.* 50-B (1954) 465–470.
- [34] R.C. Mackenzie, *Simple Phyllosilicates Based On Gibbsite And Brucite-Like Sheets. Differential Thermal Analysis*, vol. 1, Academic Press, London, 1970, (pp. 497–537).
- [35] R.C. Mackenzie, *The Differential Thermal Investigation of Clays; Mineralogical Society, Clay Minerals Group, London, 1957*, (pp. 191–206).
- [36] G. Kakali, T. Perraki, S. Tsivilis, E. Badogiannis, *Appl. Clay Sci.* 20 (2001) 73–80.
- [37] M. Alkan, C. Hopa, Z. Yilmaz, H. Guler, *Micropor. Mesopor. Mater.* 86 (2005) 176–184.
- [38] M. Al-Ghouti, M.A.M. Khraisheh, M.N.M. Ahmad, S. Allen, *J. Colloid Interf. Sci.* 287 (2005) 6–13.
- [39] Y. Bulut, H. Aydın, *Desalination* 194 (2006) 259–267.
- [40] Z. Eren, F.N. Acar, *Desalination* 194 (2006) 1–10.
- [41] H. Freundlich, *Z. Phys. Chem.* A 57 (1906) 228–304.
- [42] M. Alkan, S. Celikcapa, O. Demirbas, M. Doğan, *Dyes Pigments* 65 (2005) 251–259.
- [43] E. González-Pradas, M. Villafranca-Sánchez, A. Valverde-García, M. Socias-Viciana, *J. Chem. Tech. Biotechnol.* 42 (1988) 105–112.
- [44] L. Gómez-Jimenez, A. García-Rodríguez, J. de Dios, U. López-González, A. Navarrete-Guijosa, *J. Chem. Tech. Biotechnol.* 38 (1) (1987) 1–13.
- [45] K.R. Hall, L.C. Eagleton, A. Acrivos, T. Vermeulen, *Ind. Eng. Chem. Fundam.* 5 (1966) 212–219.
- [46] S. Tunali, A.S. Özcan, A. Özcan, T. Gedikbey, *J. Hazard. Mater.* B135 (2006) 141–148.